

A New Synthesis of Hydroxyapatite

W. Weng and J. L. Baptista

Department of Ceramics and Glasses Engineering, University of Aveiro, 3810 Aveiro, Portugal

(Received 9 July 1996; revised version received 1 October 1996; accepted 21 October 1996)

Abstract

An ethylene glycol solution of $\text{Ca}(\text{OAC})_2 \cdot x\text{H}_2\text{O}$ and a butanol solution of P_2O_5 were used as precursors to produce hydroxyapatite. Acetic acid (HOAC) and ammonium nitrate (NH_4NO_3) acted as a stabilizer and an oxidizer, respectively, during the process. A stable mixed solution of the two precursors could be obtained by adding acetic acid in the HOAC/Ca ratio of 2. As-prepared powders were obtained by pouring the mixed solution into a hot plate to evaporate the solvents. A poorly crystallized hydroxyapatite phase was obtained from the as-prepared powders after calcination at 500°C , where a dark powder was formed. Calcination at 1000°C gave white powders having a well-crystallized hydroxyapatite phase with a small amount of CaO. When NH_4NO_3 was added to the stable mixed solution before pouring into the hot plate, the as-prepared powders calcined at 500°C were white and composed of well-crystallized hydroxyapatite with a small amount of β -tricalcium phosphate. The hydroxyapatite obtained in this work is a nonstoichiometric calcium-deficient material, $\text{Ca}_{10-x}(\text{HPO}_4)_x(\text{PO}_4)_{3-x}(\text{OH})$. The described route to synthesize hydroxyapatite has potential applications for the preparation of hydroxyapatite coatings. © 1997 Elsevier Science Limited.

1 Introduction

Synthetic hydroxyapatite is a very important biomaterial used for several applications in medicine either as a bulk ceramic, a ceramic coating or as one of the components of composites. It is also used as a catalyst for the dehydration and dehydrogenation of primary alcohols. For these applications it has been found that a nonstoichiometric material is more efficient either in promoting the precipitation of biological apatite on its surface^{1,2} or in increasing the rate of the catalytic action.^{3,4} The extent of the nonstoichiometry can be evaluated through various techniques and expressed by the value of x in the formula $\text{Ca}_{10-x}(\text{HPO}_4)_x(\text{PO}_4)_{3-x}(\text{OH})$. Many routes

to synthesize hydroxyapatite have been developed using either hydrolysis,⁵ hydrothermal⁶ or precipitation methods.^{7,8} Most of these routes are based on aqueous systems. They are time-consuming and only suitable to prepare powders. Brendel⁹ developed a method to synthesize hydroxyapatite and hydroxyapatite coatings by hydrolysis and oxidation of calcium nitrate and phenyldichlorophosphine previously dissolved in acetone. Hydroxyapatite was obtained by calcination in the temperature range 700 – 1100°C . Although this method is less elaborate than the aqueous methods, the hydrolysis and oxidation steps make the procedure still relatively complicated. In a previous report we have described a suitable method to obtain hydroxyapatite by heating a mixed solution of Ca glycooxide and $\text{PO}(\text{OH})_x(\text{OR})_{3-x}$ on a hot stainless steel plate and then calcining the as-prepared powder at 1100°C .¹⁰ Although an easier method that would allow the obtainment of hydroxyapatite coatings via a sol-gel process, the high temperature necessary for the hydroxyapatite formation would preclude its application as a bioactive surface coating over some of the metal substrates used in biomedicine for bone repair. In this work we report the synthesis of hydroxyapatite using commercially available Ca acetate. We also report the way to lower the temperature of hydroxyapatite formation, describing how to get a nonstoichiometric material, $\text{Ca}_{10-x}(\text{HPO}_4)_x(\text{PO}_4)_{3-x}(\text{OH})$, at around 500 – 600°C in which HPO_4^{2-} groups ($x \neq 0$) remain after exposure to 1000°C for 1 h.

2 Experimental

Two precursor solutions, one for Ca and another for P, were first prepared. For the calcium solution, calcium acetate (Merck, dried pure) was weighed, put into a flask with ethylene glycol (Prona Lab[®] GR) and refluxed until complete dissolution. For the P solution, $\text{PO}(\text{OH})_x(\text{OBut})_{3-x}$ was used,¹¹ P_2O_5 (Riedel-deHaen, GR) was weighed, dissolved in *n*-butanol (Merck GR) and refluxed for 24 h.

Table 1. Preparation conditions of the samples studied in this work

No.	0.5 M (Ca(OAC) ₂) ₂ (ml)	4 M PO(OH) _x (OBut) _{3-x} (ml)	HOAC/Ca	NH ₄ NO ₃ /Ca
1	20.0	1.5	2	
2	20.0	1.5	2	4
3	20.0		2	
4.	As-prepared powder from sample 3*			
5	As-prepared powder from sample 1			
6	Sample 5 calcined at 500°C for 1 h			
7	Sample 5 calcined at 1000°C for 1 h			
8	As-prepared powder from sample 2			
9	Sample 8 calcined at 500°C for 1 h			

*As-prepared powder = a powder obtained by drying a solution in a hot plate at 200°C.

In this work, an 0.5 M solution of Ca acetate and a 4 M solution of PO(OH)_x(OBut)_{3-x} were used.

Because of immediate precipitation during mixing the solutions of Ca (OAC)₂ and PO(OH)_x(OBut)_{3-x}, a stable mixed solution had to be prepared by first adding acetic acid (HOAC) (GR) to the Ca acetate solution, before addition of the PO(OH)_x(OBut)_{3-x} solution. A Ca/P ratio of 1.67 was always used. The optimal ratio of HOAC to Ca was found to be 2 to get a solution stable for about a week. The stable mixed solution was poured into a hot stainless steel plate (~200°C) to evaporate the solvent and obtain powders. In a modified version of the experimental procedure, NH₄NO₃ (Merck, Crystal pure) was added to the Ca(OAC)₂ solution in order to oxidize the organic residues and its concentration tentatively optimized to the ratio NH₄NO₃/Ca of 4. When solutions with and without NH₄NO₃ were poured into the hot plate at about 200°C they behaved in different ways while

drying. The solution without NH₄NO₃ became more and more viscous and the viscous solution was finally dried to powders. The viscosity of the solution with NH₄NO₃ did not apparently change and the solvent was destroyed before the powders were formed.

For the characterization of the samples Infrared (IR), X-ray diffraction (XRD), Scanning Electron Microscopy (SEM), Energy Dispersive X-ray Spectroscopy (EDXS) and ³¹P Nuclear Magnetic Resonance (NMR) were used. The IR spectra were recorded with a Fourier transform infrared spectrometer (Nattson Galaxy 7020) with resolution of 4 cm⁻¹ using the KBr pellet method for powder samples and a liquid cell with KBr window for liquid samples. The XRD patterns were recorded with a Rigaku, D/MAX-B diffractometer with a step size of 0.05 degree for 2θ and a scan speed of 2.00 degree per minute. The morphology of the powders was observed using an Hitachi

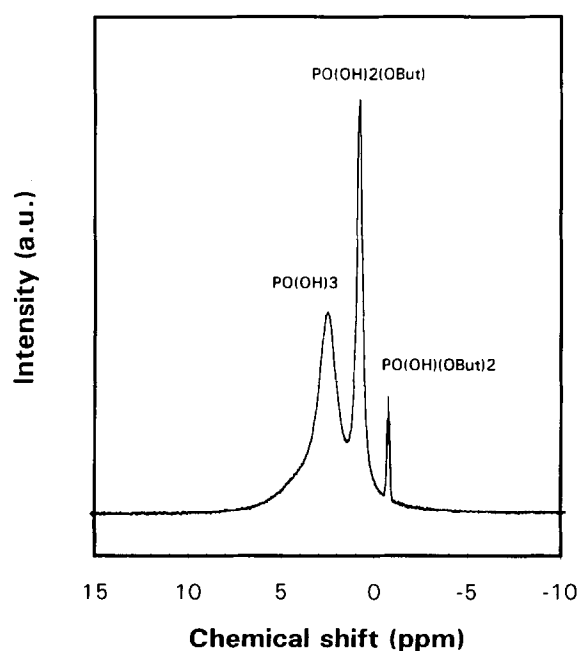


Fig. 1. ³¹P NMR spectrum of the butanol solution of PO(OH)_x(OBut)_{3-x}.

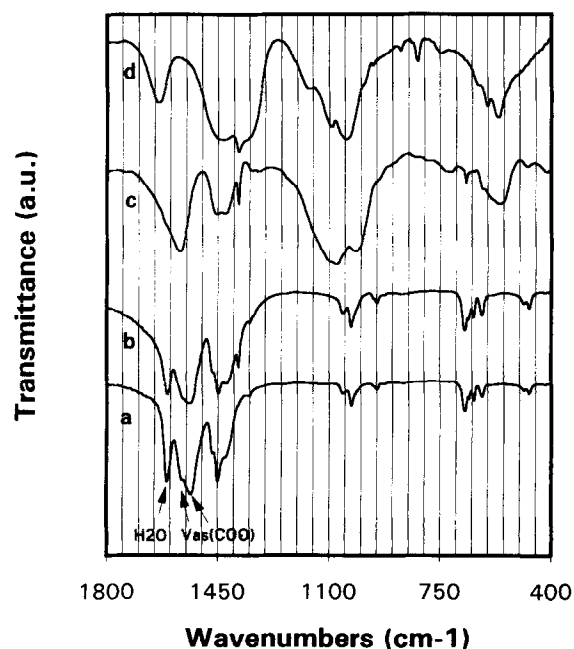


Fig. 2. IR spectra: (a) as-received Ca(OAC)₂·H₂O; (b) sample 4; (c) sample 5 and (d) sample 6.

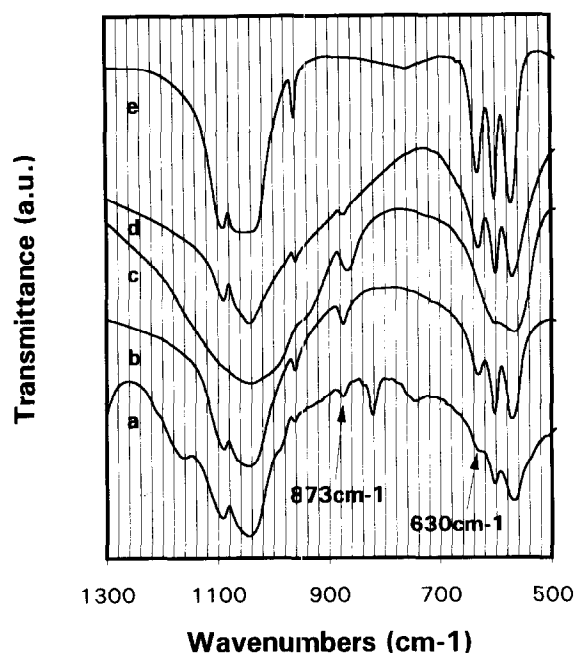


Fig. 3. IR spectra: (a) sample 8; (b) sample 10; (c) sample 5; (d) sample 6 and (e) sample 7.

S-4100 scanning electron microscope. Elemental microanalysis was performed in a Kevex EDX spectroscope with a quantum window. The region for the collected signals is estimated to be a semi-sphere with less than $1 \mu\text{m}$ diameter. The $[^{31}\text{P}]$ NMR spectrum was obtained in a Fourier transform NMR spectrometer (Bruker, AMX 300) at 300 MHz with pulse widths = $3.3 \mu\text{s}$, recycle delays = 1 s and transients = 15 K.

The preparation conditions of the samples studied in this work are listed in Table 1.

3 Results

3.1 $[^{31}\text{P}]$ NMR spectrum of the $\text{PO}(\text{OH})_x(\text{OBut})_{3-x}$ solution

The $[^{31}\text{P}]$ NMR spectrum (Fig. 1) of the solution of $\text{PO}(\text{OH})_x(\text{OBut})_{3-x}$ has three peaks at 2.5483, 0.8378 and 0.7211 ppm, which are assigned to $\text{PO}(\text{OH})_3$, $\text{PO}(\text{OH})_2(\text{OBut})$ and $\text{PO}(\text{OH})(\text{OBut})_2$, respectively, according to Ref. 11.

3.2 Powder characterization

3.2.1 IR spectra

Figures 2(a) and (b) are the IR spectra of as-received $\text{Ca}(\text{OAc})_2 \cdot \text{H}_2\text{O}$ and of sample 4. They show clearly splitting bands of $\nu_{\text{as}}(\text{COO})$ at 1570 and 1540 cm^{-1} , respectively, and an independent band of H_2O at 1610 cm^{-1} . Figure 2(c) shows that sample 5 has a broad $\nu_{\text{as}}(\text{COO})$ band at 1570 cm^{-1} which seems to include the contributions of the H_2O and acetate bands. It also shows the PO_4^{3-} bands at 1090 and 1010 cm^{-1} . Figure 2(d) from sample 8 has no sign of the acetate groups, has an H_2O

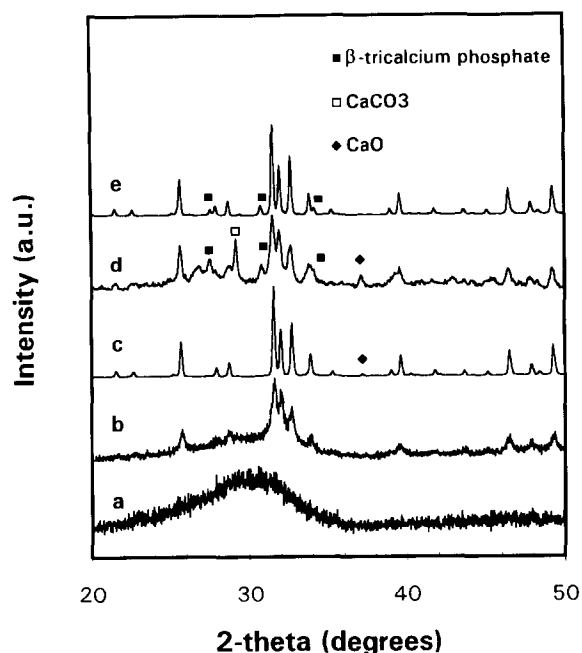


Fig. 4. XRD patterns: (a) sample 5; (b) sample 6; (c) sample 7; (d) sample 8 and (e) sample 9.

band at 1640 cm^{-1} , a broad band in the $1320\text{--}1440 \text{ cm}^{-1}$ range which possibly includes the contribution of NO_3 group at $1450\text{--}1330 \text{ cm}^{-1}$ and CO_3^{2-} groups at $1530\text{--}1320 \text{ cm}^{-1}$, and shows PO_4^{3-} band at 1170, 1090, 1040 and 960 cm^{-1} .

In Fig. 3 samples 7, 8 and 9 have a clear splitting of the 630 cm^{-1} band in 3(d),(a) and (b) which is similar to that of a commercially available hydroxyapatite powder (HAP) (Merck, 2196) in 3(e); this splitting is not observed in the IR spectrum 3(c) for sample 5.

3.2.2 XRD patterns

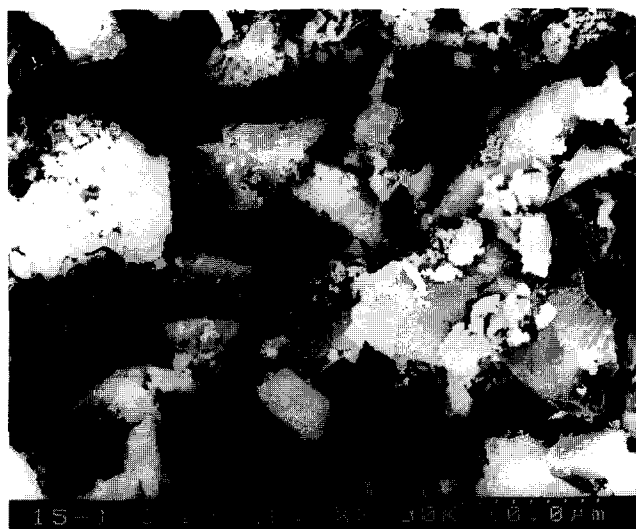
The XRD pattern of the powders obtained from the initial precursor solution without addition of NH_4NO_3 is shown in Figs 4(a), (b) and (c). Figure 4(a) shows that, after preparation, the powder (sample 5) is mainly amorphous. Calcining this powder at 500°C for 1 h shows that a poorly crystallized hydroxyapatite was already developing (Fig. 2(b)), although the powder thus obtained was black. A well crystallized hydroxyapatite, containing a small amount of CaO, could be obtained by calcination at 1000°C (Fig. 2(c)), a temperature that also allowed the obtaining of a white powder.

The as-prepared powder (sample 8) obtained from the solution with NH_4NO_3 contains mainly hydroxyapatite with some amounts of β -tricalcium phosphate, CaCO_3 and CaO phases (Fig. 4(d)). Calcination of the powder thus obtained at 500°C allowed the obtaining of a white product consisting mainly of hydroxyapatite with a small amount of β -tricalcium phosphate (Fig. 2(e)).

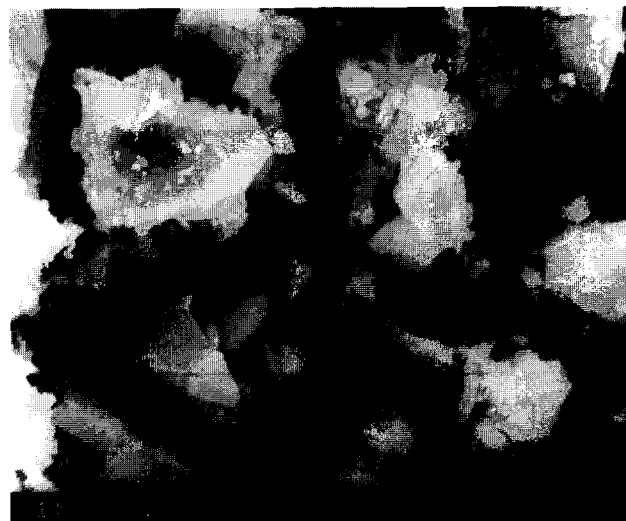
3.2.3 Morphology

The SEM micrographs of the sample are shown in Fig. 5. Figure 5(a) shows that the particles of sample 5 have a block shape which is a typical morphology of

particles obtained from smashing a xerogel. After calcination, samples 6 and 7 still keep the original shape (Figs 5(b) and (c)). It can be seen in Fig. 5(c) that each particle contains a number of fine grains.



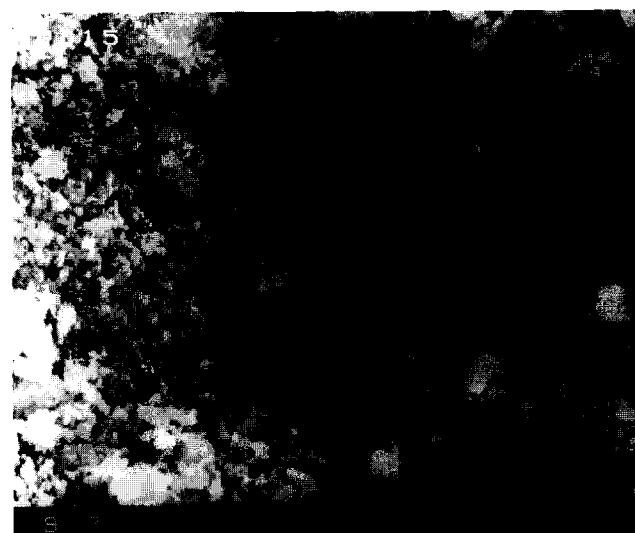
(a)



(b)



(c)



(d)



(e)

Fig. 5. SEM micrographs: (a) sample 5; (b) sample 6; (c) sample 7; (d) sample 8 and (e) sample 9.

Figures 5(b) and (e) from the samples oxidized with NH_4NO_3 show that the as-prepared powder (sample 8) is composed of small particles, which are still present in the powder after calcination (sample 9).

3.2.4 EDX results

The chemical microhomogeneity of samples 5 and 8 and of the commercial HAP powder has been checked by EDX microanalysis, analysing 10 points from different particles for each sample. The average value of the Ca/P atomic ratio is 2.00 for the three samples. The deviation from the average value is ± 0.5 for sample 5, ± 0.6 for sample 8 and ± 0.55 for the commercial powder. These are not calibrated analyses and they were performed only for comparison purposes. The considerably wide distribution of the data is probably due to the surface morphology dependence of the EDX results. They however indicate a good chemical homogeneity of the as-prepared powders in a $1\ \mu\text{m}$ scale.

4 Discussion

The IR spectra recorded for the several stages of the powder preparation by the different methods used in this work give some insight into the ways that reactions proceed.

The IR spectrum of sample 4 shows clearly the $\nu_{\text{as}}(\text{COO})$ splitting bands at 1570 and $1540\ \text{cm}^{-1}$ corresponding to the OAC ligands in both monodentate and bridging or bidentating forms.¹² The recorded pattern corresponds to that of the as-received commercial $\text{Ca}(\text{OAC})_{2,x}\text{H}_2\text{O}$ in Fig. 2(a) and indicates that in sample 4 $\text{Ca}(\text{OAC})_2$ recrystallized during heating. On the other hand the IR spectrum of sample 5 in Fig. 2(c) shows a main band in the $1570\ \text{cm}^{-1}$ region indicating that the main coordination of the acetate ligands is in a monodentate form. It also shows bands in the $1200\text{--}950\ \text{cm}^{-1}$ range which are characteristic of PO_3^{4-} .¹³ It is reasonable to consider, therefore, that the powder from sample 5 is already the product from reactions between the two precursor solutions. Otherwise the IR spectrum of sample 5 should still contain the two splitting bands of $\nu_{\text{as}}(\text{COO})$. The great increase in viscosity observed when heating the solution (sample 1) to obtain the powders (sample 5) indicates the occurrence of a gelation process. The morphology of the powder particles (Fig. 5(a)) is also typical of a gel powder. The gelation process would certainly lead to maintaining a good chemical homogeneity in the powder, as indicated by the EDX results, favoring also the reaction between the precursors to form a poorly crystallized hydroxyapatite phase at 500°C (Fig. 5(b)). The organic residues still remaining at 500°C

can only be completely removed by calcination at 1000°C and a white powder with well crystallized hydroxyapatite is obtained.

When NH_4NO_3 is added (sample 8) the IR spectrum of the as-prepared powder has no absorption band related to $\nu_{\text{as}}(\text{COO})$ but shows bands attributed to NO_3 and CO_3 groups. This implies that NH_4NO_3 has oxidized the mixture during heating. The oxidation by NH_4NO_3 seems to have completely removed the acetate ligands from the precursors, a situation that is probably favourable for them to react together leading to the formation of crystalline calcium phosphate phases during heating as seen in Fig. 4(d) in which hydroxyapatite and β -tricalcium phosphate phases can be detected together with CaCO_3 and CaO . Further reactions among β -tricalcium phosphate, CaCO_3 and CaO and residual H_2O and OH groups at 500°C lead to further formation of well crystallized hydroxyapatite in sample 9 where a lower amount of organic residues leads to the obtainment of a white powder. The small particle size of the powder of sample 8, which is still maintained in sample 9 after calcination, could be caused by the large amount of gaseous species produced and liberated during the oxidation process.

The hydroxyapatite phase obtained in this work is a calcium-deficient hydroxyapatite $\text{Ca}_{10-x}(\text{HPO}_4)_x(\text{PO}_4)_{3-x}(\text{OH})$ confirmed by the $870\ \text{cm}^{-1}$ IR spectra of Fig. 3.¹⁴ The formation of this calcium-deficient phase may result from the great number of OH groups in the P precursor as shown in Fig. 1.¹⁴

5 Conclusion

This work shows that a stable solution containing the hydroxyapatite precursors can be prepared and used to obtain, via a sol-gel method, hydroxyapatite powders at a relatively low temperature (500°C). This process can be used to prepare hydroxyapatite coatings when the nature of the substrate will be damaged by high temperature processing of the coating precursors.

References

1. Posner, A. S., Crystal chemistry of bone minerals. *Physiol. Rev.*, 1969, **49**, 760.
2. Radin, S. R. and Ducheyne, P., The effect of calcium phosphate ceramic composition and structure on in-vitro behavior, II. Precipitation. *J. Biomed. Mater. Res.*, 1993, **27**, 35.
3. Bett, J. A. S., Christener, L. G. and Hall, W. K., Hydrogen held by solids, XII. hydroxyapatite catalysts. *J. Am. Chem. Soc.*, 1967, **89**, 5535.
4. Joris, S. J. and Amberg, C. H., Nature of deficiency in nonstoichiometric hydroxyapatite, I. Catalytic activity of calcium and strontium hydroxyapatite. *J. Phys. Chem.*, 1971, **75**, 3167.

5. Mna, H., Veno, S. and Kanazawa, T., Properties of hydroxyapatite prepared by the hydrolysis of tricalcium phosphate. *J. Chem. Tech. Biotechnol.*, 1981, **31**, 15.
6. Ioku, K. and Yoshimura, M., Hydrothermal synthesis of microcrystalline apatite. *Phosphorus Lett.*, 1992, **15**, 3.
7. Moreno, E. C., Gregory, T. M. and Brown, W. M., Preparation and solubility of hydroxyapatite. *Natl Bur. Stand.*, 1968, **72a**, 773.
8. Partenfelder, U., Engel, A. and Russel, C., A pyrolytic route for the formation of hydroxyapatite/fluoroapatite solid solutions. *J. Mater. Sci.: Mater Med.*, 1993, **4**, 292.
9. Brendel, T., Engel, A. and Russel, C., Hydroxyapatite coatings by a polymeric route. *J. Mater. Sci.: Mater Med.*, 1992, **3**, 175.
10. Weng, W. and Baptista, J. L., Synthesis of Ca phosphates by $\text{PO}(\text{OH})_x(\text{OBut})_{3-x}$ and $\text{CaO}_2\text{C}_2\text{H}_4$. *J. Sol-Gel Sci. Technol.*, in press.
11. Livage, J., Barboux, P., Vandenborre, M. T., Schmutz, C. and Taulelle, F., Sol-gel synthesis of phosphate. *J. Non-Cryst. Solids*, 1992, **147&148**, 18.
12. Nakamoto, K., *Infrared and Raman Spectra of Inorganic and Coordination Compounds*, 3rd edn. John Wiley & Sons, New York, 1978, p. 237.
13. Suwa, Y., Banno, H., Mizuno, M. and Saito, H., Synthesis of compositional regulated hydroxyapatite from $\text{Ca}(\text{OH})_2$ and H_3PO_4 . *J. Ceram. Soc. Japan, Int. Edition*, 1993, **101**, 642.
14. Ishikawa, K., Ducheyne, P. and Radin, S., Determination of the Ca/P ratio in calcium-deficient hydroxyapatite using X-ray diffraction analysis. *J. Mater. Sci.: Mater Med.*, 1993, **4**, 165.